Preferential Radar Method for Dynamic Assignment of Wi-Fi Channels

Jesús David Sandoval Posso(✉)
and Carlos Andres Giraldo Castañeda(✉)

College of Engineering, Pontificia Universidad Javeriana Cali,
Valle del Cauca, Colombia
{jdposso, cgiraldoc}@javerianacali.edu.co

Abstract. A variety of methods has been developed for the optimization of channels in the bandwidth of Wi-Fi networks. Some methods will consider the existence of a single network and allow dynamic allocation of Wi-Fi channels to access points based on different criteria [1–4]. However, in many cases there is more than one Wi-Fi network and some methods were designed in this context and try to reduce the interference between access points and coexisting networks [5, 6]. This article presents a new method identified as a preferred radar algorithm (RP). The RP is based on a search algorithm that decreases the global interference of the environment for each access point. The modified ICORAL and RP methods were implemented allowing to improve the global interference of the environment. The RP and ICORAL methods were fully characterized with radar system embedded in a university environment. The RP shows a significant improvement of at least 30% more interference decrease than the ICORAL.

Keywords: Dynamic channel assignment · Cognitive radio · Wi-Fi

1 Introduction

In recent years, many wireless devices use the Internet to transmit and receive information from the network, better known as Internet of Things (IoT). It is generally based on the communication principles of the IEEE 802.11 standards, or Wi-Fi network [6]. The number of wireless devices has increased significantly and has generated channel allocation problems and optimization of the use of the 2.4 GHz band. The Bluetooth, Wi-Fi, NFC and ZigBee protocols have extended spectrum techniques in the 2.4 GHz band [7]. To minimize this problem, several approaches have been proposed, seeking dynamic solutions that optimize the ISM band. Among these techniques is the Dynamic Allocation of Cisco DCA Channels, which is taking decisions of channel change according to the historical study of the behavior of the network and some improvement parameters [2]. The dynamic allocation of multi-factor MFDCA channels [8], propose a focus on energy efficiency and the channel width adaptation algorithm seeks to reduce interference and improve transfer speed [9]. However, these techniques assume the existence of a single network where all the access points belong to it and it is not considered that more than one network can coexist in the environment.

A. Kliks et al. (Eds.): CrownCom 2019, LNICST 291, pp. 87–99, 2019.
https://doi.org/10.1007/978-3-030-25748-4_7

Some techniques approach the problem where several networks interact in the same medium. As it is the case of the coral algorithm [3] the latter monitors the network with a mobile unit and reassigns the non-overlapping frequency channels of the 2.4 GHz band generated coral shaped structures in populations of access points in channels 1, 6 and 11. In this article, we present a method where the allocation of channels is independent of the networks that coexist in the medium. The method is based on cognitive radio and makes use of radar external to the networks that monitors the medium 360° and locates the access points referring to it for the reassignment of channels, decreasing the global interference. This new method is called the preferred radar algorithm.

2 Methods of Channel Dynamic Assignment

2.1 Improved Coral Algorithm (ICORAL)

The methodology of the improved coral algorithm is based on the principle of assigning each access point a channel without spectral overlap. This is achieved by maintaining a 5-channel difference between assigned access points. The rules that govern the method are described below. The flow chart of the preferred radar method is shown in Fig. 1.

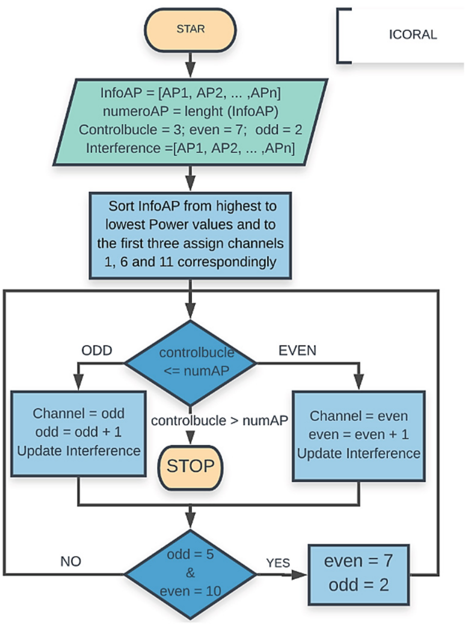

Fig. 1. Flow diagram of the ICORAL dynamic assignment method.

Rules of the ICORAL methodology:

1. Sort from highest to lowest power the APs monitored by the radar.
2. Non-overlapping frequency channels are assigned in 1, 6 and 11 to the APs of greater power with respect to the radar.
3. For the following APs, pairs of non-interfering channels (2,7), (3,8), (4, 9) and (5,10) are assigned.
4. A new evaluation of the next AP to be studied is started and the process from step 2 onwards is repeated until analyzing all the APs registered by the radar.

2.2 Preferential Radar Algorithm RP

The methodology of the preferential radar algorithm is based on the principle of assigning to each access point a channel that minimizes the impact of global interference of the operating environment and independent of the network to which it belongs. The rules that govern the method are described below. The flow chart of the preferred radar method is shown in Fig. 2.

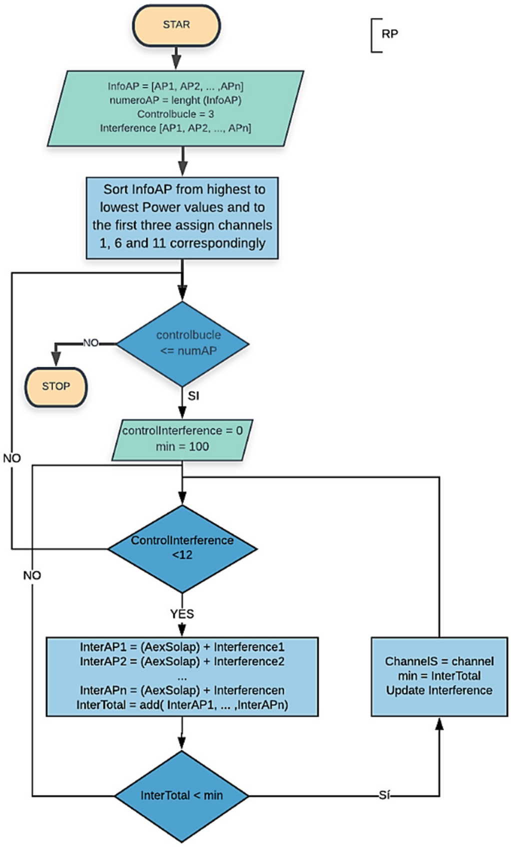

Fig. 2. Flow diagram of the RP dynamic assignment method.

Rules of the RP methodology:

1. Sort from highest to lowest power the APs monitored by the radar.
2. Non-overlapping frequency channels are assigned in 1, 6 and 11 to the APs of greater power with respect to the radar.
3. For the following APs, the cumulative interference metric of each of the Wi-Fi band channels with the ancestors already assigned to the environment is studied.
4. The value of the accumulated interference generated by each channel is stored and the channel with the least interference weight in the environment is identified so that it is assigned to the AP studied.
5. A new evaluation of the next AP to be studied is started and the process from step 3 onwards is repeated until analyzing all the APs registered by the radar.

3 Accumulated Interference Model

Taking as reference the interference model of several methods of dynamic channel allocation where the interference is modeled as the sum of the multiplication of two factors, such as RSSI and COIC (Dynamic channel assignment) [1, 3, 5, 6, 8] and based on this principle our cumulative interference model is defined as:

$$In_{i,j} = \sum_{j=1}^{n} ASC_{i,j} \times SFR_{i,j} \tag{1}$$

Where: $In_{i,j}$: cumulative interference of the access point, $ASC_{i,j}$: area of overlap in coverage between adjacent APS, $SFR_{i,j}$: spectral overlap of Wi-Fi channels.

4 APs Coverage Area

The radioelectric balance is carried out using Recommendation ITU-R P.1238-9 (06/2017) [10]. This recommendation uses propagation data and prediction methods in the planning of indoor radiocommunication systems and local area radiocommunication networks in the frequency range 900 MHz to 100 GHz. The recommendation is used in the Wi-Fi band. The model proposed by the ITU considers some coefficients of power loss due to distance such as transmission through walls, obstacles, loss factors that can manifest in single-floor buildings among others. In order to simplify the problem. The basic model for losses based on distance is illustrated below:

$$L_{total} = 20log_{10}(f) + Nlog_{10}(d) + L_f(n) - 28 \tag{2}$$

Where: N: Coefficient of power loss due to distance. See Table 1, f: frequency (MHz), d: separation distance (m) between the base station and the portable terminal (where d > 1 m), Lf: soil penetration loss factor (dB). See Table 2, n: number of floors between the base station and the portable terminal (n $\geq$ 1).

Table 1. Coefficient of loss of power, N, for the calculation of the loss of transmission in interiors. [11].

Frequency (GHz)	Residential building (dB)	Office building (dB)	Commercial building (dB)
0,9	-	33	20
2,4	28	30	-
5,2	-	31	-
5,8	-	24	-

Table 2. Ground penetration loss factors, Lf (dB), being the number of floors penetrated, for the calculation of the transmission loss in interiors ($n \geq 1$) [11].

Frequency (GHz)	Residential building (dB)	Office building (dB)	Commercial building (dB)
0,9	-	9 (1 floor) 19 (2 floor) 24 (3 floor)	-
2,4	10 (apartment) 5 (home)	14	-
5,2	13 (apartment) 7 (home)	16 (1 floor)	-
5,8	-	22 (1 floor) 28 (2 floor)	-

For the calculation of the coverage distance, omnidirectional propagation antennas are assumed with dipole antennas G = 1.68, transmission powers of 20 mW and reception sensitivity −80 dBm for all the APs monitored by the radar. The ASC factor is calculated as a measure of the interception between adjacent APs coverage areas as shown in Fig. 3.

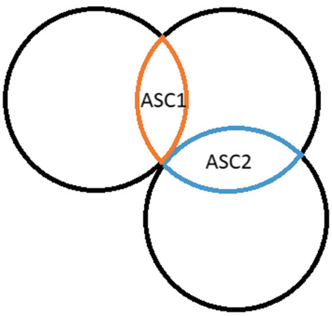

Fig. 3. Overlapping coverage area.

5 Spectral Overlap of Wi-Fi Channels

The SFR factor is obtained by observing the Wi-Fi channel distribution monitored by the radar. Where it is observed that a separation of 5 channels is necessary so that there is no spectral overlap. As the separation between channels decreases the percentage of overlap increases as observed in Table 3 and Fig. 4.

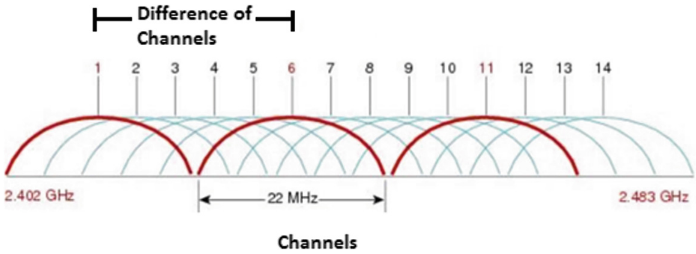

Fig. 4. Channels Wi-Fi.

Table 3. Overlap frequency in channel Wi-Fi.

Difference between channels	Overlap %
0	100
1	77,27
2	55,55
3	31,82
4	9,09
>5	0

6 System Design

In Fig. 5, the system is illustrated in a block diagram in which the computer controls the whole system and sends an order to the Wi-Fi module so that the signals are captured by means of the antenna of the access points (initial position of the radar). The scanning is performed several times in order to validate the acquired signals. After the first scan, the PC sends the turn command to the motor controller so that it moves 10 degrees counterclockwise until it goes full circle and concludes the monitoring of the radar environment. When finishing with the location of the access points the user interface draws the environment and locates each access point and its respective coverage area according to the standard established in the ITU-R P.1238-9 (06/2017) of the Wi-Fi radio link [10, 12].

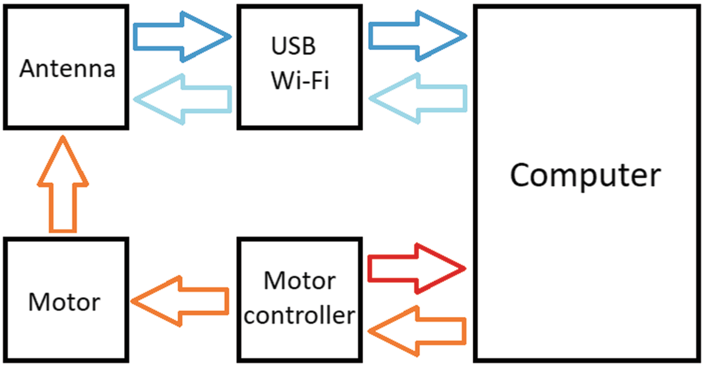

Fig. 5. System block diagram.

Figure 6 shows the global system with each of its parts. The pieces that make up the comet 17 radar are: 1. Antenna Ettus LP0965, 2. Base for the antenna, 3. Base for switch, 4. Coupling of the motor shaft, 5. Switch, 6. Stepper Motor, 7. Arduino Uno, 8. USB - Wi-Fi, 9. Power driver for Step-Step motor, 10. First level of the frame, 11. Frame cover, 12. Second level of the frame

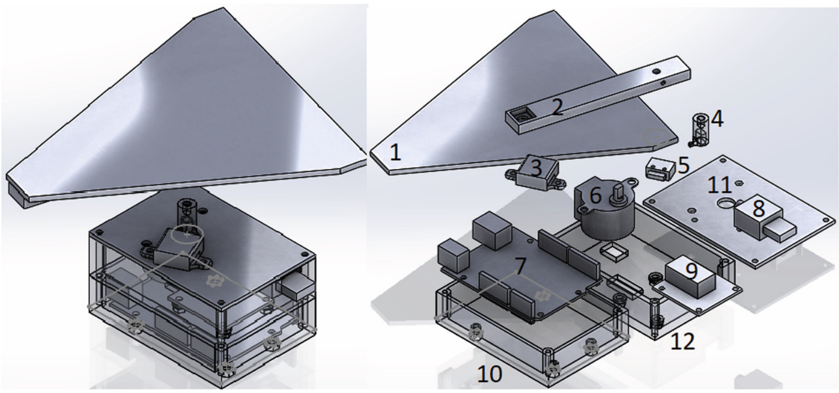

Fig. 6. Radar Comet and radar break down.

In the block diagram, there is the block of the antenna that is represented in the exploded view of the radar as item number 1. Directional logarithmic PCB antenna with gain of 6 dBi and a bandwidth from 850 MHz to 6.5 GHz [13]. The Wireless-N 150Mbps reference adapter is located in the USB-Wi-Fi block. It has a Realtek 8188CU reference chipset that accepts the IEEE802.11 n, g and b, part number 8. The pieces number 5, 7 and 9 refer to the motor controller block in the block diagram, which consists of an Arduino Uno, a switch to determine the mechanical zero and a ULN2003 drive with 5–12 VDC power and a maximum output of 500 mA [14] Piece number 6 refers to the engine block. 28BYJ-48 motor with 5 VDC power supply with 4 phases and a 1/64 gearbox [15].

7 User Interface

Figure 7 shows the user interface of the system. The left section visualizes the environment monitored by the radar where the current status of the APs with their respective coverage areas and Wi-Fi operation channel is observed. Each color is associated with a specific channel of the bandwidth. The right section shows the changes of the environment when executing the algorithms of dynamic allocation of channels. In this case, the new channel distribution of the APs is observed when executing the preferential radar algorithm.

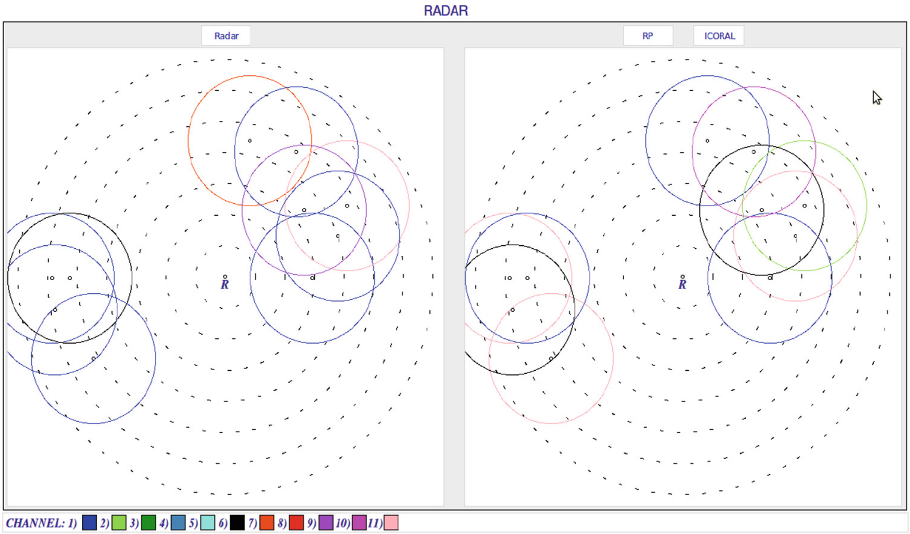

Fig. 7. Scenario of an environment and dynamic channel allocation using RP.

8 Experimental Results

The experimental tests of the radar prototype were carried out at the Pontificia Universidad Javeriana Cali, in the buildings of Lago and Palmas where many APs belonging to different Wi-Fi networks interact. The methodology for conducting the tests consisted of making 10 sweeps in a fixed position of the building and calculating the measure of the accumulated interference. Each method of dynamic allocation was tested under the same conditions. The objective was to characterize them and evaluate their performance based on the same cumulative interference metric with the environment. Next, the results are displayed. Lago building tests:

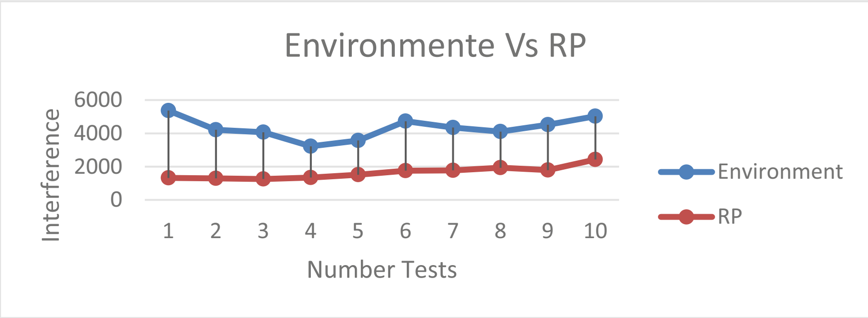

Fig. 8. Comparison of the environment with dynamic assignment of RP channels.

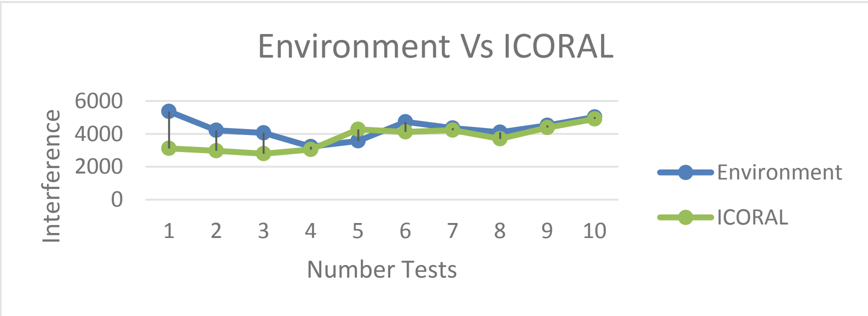

Fig. 9. Comparison of the environment with the dynamic channel assignment ICORAL.

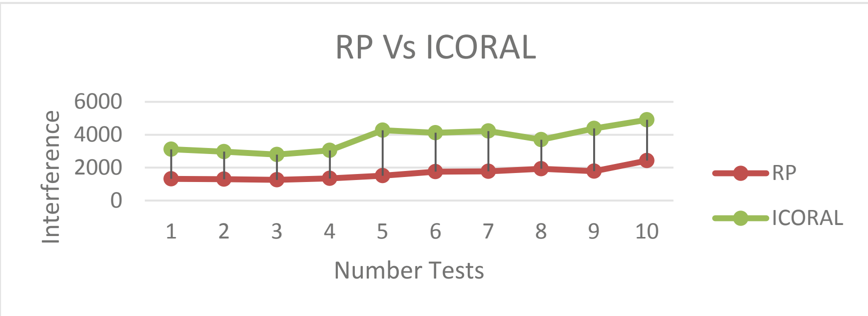

Fig. 10. Comparison of the two methods of dynamic allocation of RP Vs channels ICORAL.

Figures 8 and 9 show the behavior of the cumulative interference with the environment for both methods in the Lago building. The RP algorithm in all tests significantly improves the interference. While the ICORAL algorithm improves in the first three tests but remains almost equal to the environment in the others. Comparing the RP and ICORAL algorithms in Fig. 10 it is observed that RP has a significant improvement in interference over ICORAL for all tests.

Table 4. Ratio of improvement between the methods of dynamic allocation of channels and the environment (Lago Building).

Test	Environment *(I)*	Methods		Improvement ratio	
		RP *(I)*	ICORAL *(I)*	RP	ICORAL
1	5364	1320	3116	0,75	0,42
2	4216	1298	2972	0,69	0,30
3	4064	1258	2792	0,69	0,31
4	3222	1346	3048	0,58	0,05
5	3572	1512	4274	0,58	−0,20
6	4728	1756	4124	0,63	0,13
7	4348	1778	4226	0,59	0,03
8	4104	1934	3698	0,53	0,10
9	4514	1788	4384	0,60	0,03
10	5026	2430	4910	0,52	0,02
Average				0,62	0,12

Table 4 shows the summary of the tests carried out in the Lago building. It is observed that the methods of allocation of RP and ICORAL channels have an improvement of the average environment of 62% and 12% respectively regarding the interference of the environment. Palmas building tests:

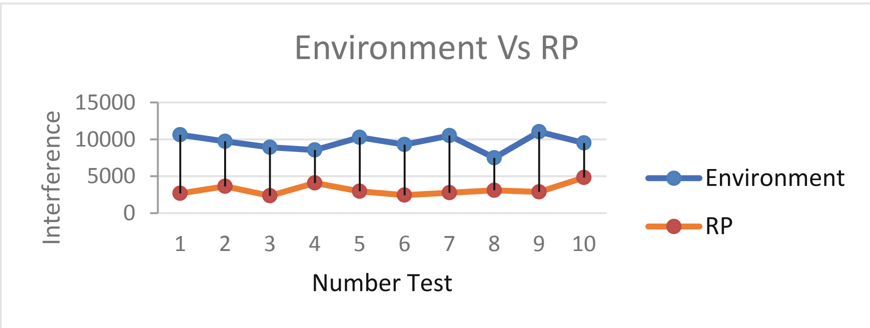

Fig. 11. Comparison of the environment with dynamic allocation of RP channels.

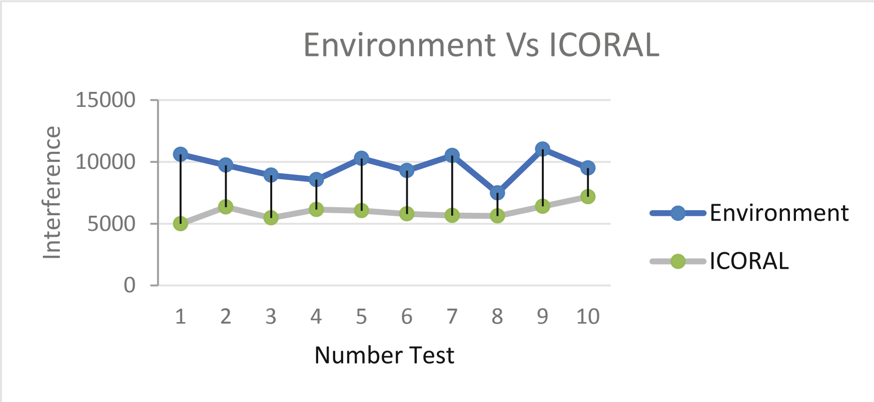

Fig. 12. Comparison of the environment with the dynamic allocation of channels ICORAL.

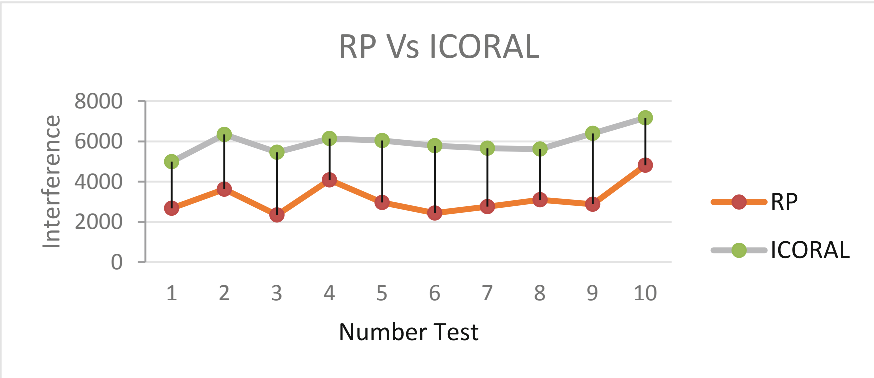

Fig. 13. Comparison of the two methods of dynamic allocation of RP Vs channels ICORAL.

Figures 11 and 12 show the behavior of the accumulated interference with the environment for both methods in the Palmas building. Both RP and ICORAL algorithms greatly improve the interference in all tests. Comparing the RP and ICORAL algorithms in Fig. 13 it is observed that RP has a better behavior in interference with respect to the ICORAL for all the tests.

Table 5. Ratio of improvement between the methods of dynamic allocation of channels and the environment (Palmas Building).

Test	Environment *(I)*	Methods		Improvement ratio	
		RP *(I)*	ICORAL *(I)*	RP	ICORAL
1	10602	2676	4992	0,75	0,53
2	9730	3626	6344	0,63	0,35
3	8918	2344	5460	0,74	0,39
4	8562	4086	6142	0,52	0,28

(*continued*)

Table 5. (*continued*)

Test	Environment *(I)*	Methods		Improvement ratio	
		RP *(I)*	ICORAL *(I)*	RP	ICORAL
5	10276	2966	6042	0,71	0,41
6	9288	2436	5786	0,74	0,38
7	10510	2760	5656	0,74	0,46
8	7486	3096	5618	0,59	0,25
9	11022	2878	6398	0,74	0,42
10	9498	4814	7174	0,49	0,24
Average				0,66	0,37

Table 5 shows the summary of the tests carried out in the Palmas building. It is observed that the methods of allocation of RP and ICORAL channels have an improvement of the average environment of 66% and 37% respectively regarding the interference of the environment.

9 Conclusions

A radar-based Wi-Fi access point monitoring system was developed. The objective was to evaluate the methods of dynamic allocation of Preferential Radar (RP) and Improved Coral (ICORAL) channels against interference. The methods were completely characterized with a series of tests in different buildings. The tests allowed to observe the behavior of the methods with respect to the accumulated interference of the environment.

The results show that both ICORAL and RP methods improve on average between 30% and 63% the accumulated interference of the environment respectively. The ICORAL algorithm in some cases behaved in the face of interference in a similar way to the environment. The performance of the RP method significantly improved the interference of the environment in all the tests carried out. Comparing the methods, it is observed that the RP method has 33% better performance against interference than the ICORAL method.

References

1. Zhao, Y., Wu, Y., Feng, Y., Zheng, Y., Fang, X.: Dynamic channel selections and performance analysis for high-speed train WiFi network, pp. 1–5. IEEE, Xi'an (2015)
2. CISCO DCA. https://www.cisco.com/c/en/us/td/docs/wireless/controller/technotes/8-3/b_RRM_White_Paper/b_RRM_White_Paper_chapter_0100.pdf. Accessed 12 Jan 2019
3. Wang, B., Wu, W., Liu, Y.: Dynamic channel assignment in wireless LANs, pp. 12–17. IEEE, China (2008)
4. Chang, C.-Y., Chang, C.-T., Huang, P.C.: Dynamic channel assignment and reassignment for exploiting channel reuse opportunities in ad hoc wireless networks, vol. 2, pp. 1053–1057. IEEE, Singapore (2002)

5. Mack, J., Gazor, S., Ghasemi, A., Sydor, J.: Dynamic channel selection in cognitive radio WiFi networks: an experimental evaluation, pp. 261–267. IEEE, Sydney (2019)
6. Mathur, K., Jena, D., Agrawal, S., Baburaj, S., Kondabathini, S., Tyagi, V.: Throughput improvement by using dynamic channel selection in 2.4 GHz band of IEEE 802.11 WLAN, pp. 805–810. IEEE, Prague (2018)
7. Kobayashi, H., Kameda, E., Shinomiya, N.: A matching-based strategy for AP selection in sustainable heterogeneous wireless networks. In: ISCC 2016, pp. 103–107. IEEE (2016)
8. Ribeiro, L., Souto, E., Becker, L.B.: Multi-factor dynamic channel assignment approach for Wi-Fi networks. In: IEEE Symposium on Computers and Communications (ISCC), pp. 1–7 (2018)
9. Ni, C., Gan, C., Ma, X., Wu, C.: Dynamic bandwidth allocation with optimized excess bandwidth distribution and wavelength assignment in multi-wavelength access network. In: International Conference of IEEE Region 10, TENCON 2013, pp. 1–4. IEEE, China (2013)
10. Recommendation ITU-R P.1238-9 (06/2017). https://www.itu.int/dms_pubrec/itu-r/rec/p/R-REC-P.1238-9-201706-I!!PDF-E.pdf
11. Leslye, C., Andrea, J., Marco, M.: Métodos de diseño y cobertura para redes wifi indoor y outdoor, caso UTPL, pp. 1–7. Academia, Ecudor (2013)
12. Pozar, D.: Microwave Engineering, 3rd edn. Wiley, New York (2005)
13. KB ETTUS. https://kb.ettus.com/images/0/06/ettus_research_lp0965_datasheet.pdf
14. Datasheet ULN2003. https://www.electronicoscaldas.com/datasheet/ULN2003A-PCB.pdf
15. Datasheet Stepper Motor. http://robocraft.ru/files/datasheet/28BYJ-48.pdf